Biol Blood Marrow Transplant 20 (2014) 37–45

Rejection of Leukemic Cells Requires Antigen-Specific T Cells with High Functional Avidity

Krystel Vincent [1,2], Marie-Pierre Hardy [1,2], Assya Trofimov [1,2], Céline M. Laumont [1,2], Dev Sriranganadane [1,3], Sarah Hadj-Mimoune [1,2], Insaf Salem Fourati [4], Hugo Soudeyns [4], Pierre Thibault [1,3], Claude Perreault [1,2,*]

[1] *Institute for Research in Immunology and Cancer, Université de Montréal, Montréal, Quebec, Canada*
[2] *Department of Medicine, Université de Montréal, Montréal, Quebec, Canada*
[3] *Department of Chemistry, Université de Montréal, Montréal, Quebec, Canada*
[4] *Department of Microbiology, Infectiology and Immunology, Université de Montréal, Montréal, Quebec, Canada*

Article history:
Received 5 September 2013
Accepted 21 October 2013

Key Words:
CD8 T lymphocyte
Leukemia-associated antigen
Leukemia immunotherapy
Major histocompatibility complex
Minor histocompatibility antigen

A B S T R A C T

In a context where injection of antigen (Ag)-specific T cells probably represents the future of leukemia immunotherapy, identification of optimal target Ags is crucial. We therefore sought to discover a reliable marker for selection of the most potent Ags. To this end, (1) we immunized mice against 8 individual Ags: 4 minor histocompatibility Ags (miHAs) and 4 leukemia-associated Ags (LAAs) that were overexpressed on leukemic relative to normal thymocytes; (2) we assessed their ability to reject EL4 leukemic cells; and (3) we correlated the properties of our Ags (and their cognate T cells) with their ability to induce protective antileukemic responses. Overall, individual miHAs instigated more potent antileukemic responses than LAAs. Three features had no influence on the ability of primed T cells to reject leukemic cells: (1) MHC-peptide affinity; (2) the stability of MHC-peptide complexes; and (3) epitope density at the surface of leukemic cells, as assessed using mass spectrometry. The cardinal feature of successful Ags is that they were recognized by high-avidity CD8 T cells that proliferated extensively in vivo. Our work suggests that in vitro evaluation of functional avidity represents the best criterion for selection of Ags, which should be prioritized in clinical trials of leukemia immunotherapy.

INTRODUCTION

Allogeneic hematopoietic cell transplantation (AHCT) led to the discovery of the allogeneic graft-versus-leukemia (GVL) effect, which remains the most convincing evidence that immune cells can cure cancer in humans [1-3]. After conventional HLA-matched AHCT, GVL is clearly mediated by donor T cells that use several cytotoxic mechanisms to kill leukemic cells [4-8]. T cells from an allogeneic (nonidentical twin) HLA-matched donor can react to both leukemia-associated Ags (LAAs) and minor histocompatibility Ags (miHAs) on recipient cells, whereas an identical twin (syngeneic) donor can react to LAAs but not miHAs. miHAs are polymorphic MHC-associated peptides that result from genetic variations such as single nucleotide polymorphisms [9-12]. Strikingly, in mice and humans, the GVL effect is abrogated when the donor is syngeneic. There is, therefore, general agreement that after conventional AHCT, the GVL effect depends on direct recognition of host miHAs by donor T cells [1,2,8,13-19].

Nonetheless, even though the GVL effect after conventional AHCT is clearly miHA dependent, evidence suggests that LAAs are immunogenic and might contribute to GVL initiated by miHA-responsive T cells. Expansion of donor T cells specific for PR1 and WT1 was observed post-AHCT, and, in the case of WT1, correlated with the occurrence of GVL [20,21]. Moreover, evidence suggests that miHA-triggered GVL initiates Ag spreading that leads to T cell responses against LAAs [2]. Finally, overall comparisons between miHAs and LAAs may not be fair. Though exact numbers are not known, estimates suggest that the number of different miHAs that can be recognized by allogeneic T cells may be as high as 100 [12,22], whereas the number of immunogenic LAAs expressed by a population of leukemic cells is probably less than 10 [23,24]. Therefore, GVL might appear to be dependent on miHAs simply because donor T cells are confronted with a larger repertoire of miHAs than LAAs. Consequently, there is no evidence that on a per Ag basis, there are differences in the antileukemic activity of T cells targeted to LAAs versus miHAs [25,26]. In a context where injection of Ag-specific T cells probably represents the future of leukemia immunotherapy [2], identification of the best targets is of capital importance. If, on a per Ag basis, LAAs are as effective as miHAs, then targeting LAAs would be preferable because autologous T cells could be used. The superiority of miHAs would require the use of allogeneic donors. The goal of the present work was, therefore, to investigate the rules determining whether an Ag (miHA or LAA) is a good target for leukemia immunotherapy. We sought to directly address this question using a straightforward approach: (1) we immunized mice against 8 individual Ags (4 miHAs and 4 LAAs), and we then assessed their ability to reject EL4 leukemic cells; and (2) we compared the properties of these Ags (and their cognate T cells) to discover which features correlated with antileukemic activity in vivo. To the best of our knowledge, our work provides the first direct comparison of antileukemic responses induced by individual miHAs and LAAs. We report that, overall,

Financial disclosure: See Acknowledgments on page 44.

* Correspondence and reprint requests: Claude Perreault, Institute for Research in Immunology and Cancer, Université de Montréal, P.O. Box 6128, Station Centre-ville, Montréal, QC, Canada H3C 3J7.
E-mail address: claude.perreault@umontreal.ca (C. Perreault).

1083-8791/$ – see front matter © 2014 American Society for Blood and Marrow Transplantation.
http://dx.doi.org/10.1016/j.bbmt.2013.10.020

individual miHAs generated much more potent antileukemic responses than LAAs. In vivo antileukemic activity was dictated by the functional avidity of Ag-reactive T cells and not by epitope density on leukemic cells nor by the strength of peptide-MHC (pMHC) interactions.

MATERIALS AND METHODS

Mice

B10.C-H7^b/Sn (B10.H7^b), B10.LP- H3^b H13^b/(36NS)Sn (B10.H3^b/H13^b), B10.129P-H46^b H47^b/(21M)Sn (B10.H4^b), C57BL/10J (B10) and C57BL/6 (B6) mice were obtained from The Jackson Laboratory (Bar Harbor, ME). B10.H7^b, B10.H3^b/H13^b, and B10.H4^b mice are referred to as B10-congeneic mice. Mice were housed under specific pathogen-free conditions and all experimental protocols were approved by the Comité de Déontologie de l'Expérimentation sur des Animaux of Université de Montréal.

Peptides

Native peptides and FITC-conjugated peptides (SII[Lys-FITC]FEKL) and (ASP[Lys-FITC]NSTVL) were synthesized by GenScript (Piscataway, NJ). Purity, as determined by the manufacturer, was greater than 95%. ^{13}C-versions of VAAANR*EVL, STLTYSR*M and KAPDNR*ETL peptides were synthesized by JPT Peptide Technologies (Berlin, Germany).

Cell Lines

The EL4 lymphoma cell line was obtained from the American Type Culture Collection (Manassas, VA) and was cultured in DMEM supplemented with 10% horse serum. RMA-S cells, provided by Dr. Sylvie Lesage (Université de Montréal), were cultured in RPMI 1640 medium supplemented with 10% fetal bovine serum and .048 mmol/L β-mercaptoethanol. Cell cultures were supplemented with 2 mmol/L L-glutamine and 2 mmol/L penicillin-streptomycin.

Preparation of Bone Marrow–derived Dendritic Cells (DCs), Mouse Immunization, and Survival Curves

Bone marrow–derived DCs were generated as previously described [27]. For mouse immunization, DCs from male mice were pulsed with the selected peptide (2 μM) for 3 hours. Cells were washed and injected i.v. (10^6 cells per mice) in 8- to 16-week-old female mice on day -14 and day -7. On day 0, EL4 cells were harvested, washed 3 times in PBS, and injected i.v. Mice were monitored for loss of weight, paralysis, or tumor outgrowth. B10-congeneic and B6 female mice were used to generate miHA- and LAA-specific CD8 T cells, respectively. As negative controls, B6, B10, or B10-congeneic female mice were immunized with unpulsed DCs derived from syngeneic mice.

Cell Sorting, Flow Cytometry, and Cytotoxicity Assays

For cell sorting, 30×10^6 splenocytes/mL were stained with FITC-labeled anti-CD8a (53–6.7; BD Bioscience). Splenocytes were stained for 30 minutes at 4°C, washed, and sorted using a FACSAria apparatus. MHC I tetramers were provided by the NIH tetramer core facility (Atlanta, GA). For tetramer labeling, sorted CD8 T cells were stained with 2.5 μg/10^6 cells of the appropriate APC-labeled MHC class I tetramer for 15 minutes at 37°C prior to flow cytometry. Two negative controls were analyzed: (1) staining of naïve cells with the relevant tetramer, and (2) staining of primed cells with an irrelevant tetramer. Since both controls showed similar background staining, we present only staining of naïve cells with the relevant tetramer as a negative control. Analyses were performed on a BD Canto II flow cytometer using FACSDiva software (BD Bioscience; Mississauga, ON, Canada). In vitro cytotoxicity assays were performed as previously described, with minor modifications [28]. Splenocytes harvested from immunized mice were depleted of natural killer cells using a biotinylated anti-NK1.1 antibody (Ab) (PK136; BD Bioscience) and the EasySep mouse biotin positive selection kit (Stem Cell Technologies). The remaining cells were restimulated in vitro in complete RPMI with 2 μM of the relevant peptide for 5 days and used as effectors. Target cells were CFSE-stained EL4 cells. Effector and target cells were incubated at different ratios overnight and analyses were performed on a BD LSR II flow cytometer using FACSDiva. The percentage of specific lysis was calculated as follows: ([number of remaining CFSE$^+$ cells after incubation of target cells alone minus number of remaining CFSE$^+$ cells after incubation with effector cells]/number of CFSE$^+$ cells after incubation of target cells alone) × 100.

MHC Binding Affinity and Half-life pMHC Complexes

Generation of pMHC complexes is deficient in RMA-S cells because these cells do not express functional transporter associated with Ag processing. However, at reduced temperatures (26°C) RMA-S cells express empty, peptide-receptive, MHC class I molecules. These cells can, therefore, be used to load specific peptides on MHC molecules to create pMHC complexes that remain stable at 37°C [29]. For the evaluation of peptide binding to H2D^b and H2K^b, RMA-S cells were incubated overnight at 26°C, pulsed with 10^{-10} to 10^{-4} M of the selected peptide, incubated at 37°C for 2 hours, washed, and stained with Abs against MHC I molecules. For assessment of MHC binding affinity, RMA-S cells were pulsed with the test peptide and 10^{-7} M of FITC-conjugated competitor peptide. After incubation at 37°C for 1 hour, cells were washed and analyzed by flow cytometry to evaluate displacement of the FITC-conjugated peptide by the unlabeled peptide. To evaluate the half-life of pMHC complexes, RMA-S cells were incubated overnight at 26°C with 50 μM of the selected peptide. On the following morning, cells were washed, incubated at 37°C, stained for MHC I molecules, and analyzed by flow cytometry every hour for 12 hours. MHC staining was performed using Abs against H2D^b (B22–249.R1; Cedarlane, Hornby, ON, Canada) or H2K^b (Y3; ATCC, Manassas, VA). Cell aliquots were stained with biotin-labeled anti-IgG2a-k, (8.3; BD Bioscience) and PE-conjugated streptavidin (BD Bioscience) for H2D^b, and with FITC-conjugated anti-IgG2b-k (R12-3; BD Bioscience) for H2K^b. Half-life of pMHC complexes and affinity of peptides for MHC I molecules were estimated using a 1-phase exponential decay equation and a dose-response curve, respectively [30,31].

ELISpot and Avidity Assays

Millipore MultiScreen PVDF plates were permeabilized with 35% ethanol, washed, and coated overnight using the Mouse IFN-γ ELISpot Ready-SET-Go! reagent set from e-Bioscience (San Diego, CA). After 16 hours, sorted CD8 T cells from immunized and nonimmunized mice were plated and incubated at 37°C for 48 hours in the presence of irradiated splenocytes from syngeneic mice pulsed with the relevant peptide (4 μM for the ELISpot assay and 10^{-4} to 10^{-14} M for the avidity assay). As a negative control, CD8 T cells from naïve mice were incubated with peptide-pulsed splenocytes. Spots were revealed using the reagent set manufacturer protocol and were enumerated using an ImmunoSpot S5 UV Analyzer (Cellular Technology Ltd, Shaker Heights, OH). IFN-γ production was expressed as the number of spot-forming cells per 10^6 cells and the EC_{50} was calculated using a dose-response curve.

Peptide Quantification

MHC I–associated peptides were eluted from the cell surface of 500×10^6 EL4 cells by mild acid elution as previously described [32]. Eluates were spiked with 500 fmoles of each ^{13}C-labeled synthetic peptide, desalted on an HLB cartridge 30 cc, filtered with a 3000 Da cut-off membrane and separated into 7 fractions by strong cation exchange SpinTips (Protea Bioscience). Fractions were resuspended in .2% formic acid and analyzed by LC-MS/MS using an Eksigent LC system coupled to an LTQ-Orbitrap ELITE mass spectrometer (Thermo Fisher Scientific). Peptides were separated on a custom C18 reversed phase column (150 μm i.d. X 100 mm, Jupiter Proteo 4 μm, Phenomenex) using a flow rate of 600 nL/minute and a linear gradient of 3% to 60% aqueous ACN (.2% formic acid) in 120 minutes. Full mass spectra were acquired with the Orbitrap analyzer operated at a resolving power of 30,000 (at m/z 400). Mass calibration used an internal lock mass (protonated (Si(CH3)2O))6; *m/z* 445.120029) and mass accuracy of peptide measurements was within 5 parts per million. MS/MS spectra were acquired at higher energy collisional dissociation with a normalized collision energy of 35%. Up to 12 precursor ions were accumulated to a target value of 50,000 with a maximum injection time of 300 ms and fragment ions were transferred to the Orbitrap analyzer operating at a resolution of 15,000 at *m/z* 400. The peptide quantification protocol was adapted from Anthony W. Purcell et al. [33]. Briefly, Excalibur software (Thermo Science) was used to extract both light (endogenous) and heavy forms (^{13}C-labeled) of peptides ion mass chromatogram from mass spectrometry raw files generated from different samples. Absolute quantification was calculated using the following formula: ([Light area under peak/Heavy area under peak] × [500 fmoles of ^{13}C-labeled synthetic peptides x Avogadro's number]) / cell number.

Statistical Analysis

Results are expressed as means ± SD. Statistical significance was tested using parametric and nonparametric tests. *P* values < .05 were considered statistically significant.

RESULTS

Experimental model

We used the EL4 T-lymphoblastic leukemia cell line that originated from a C57BL/6 (B6) mouse. Amino acid sequences of several B6 miHAs were elucidated by us and others, including H3^a, H4^a, H7^a and H13^a, which were used in this

study [34-39]. In addition, we studied 4 LAAs, which were shown by mass spectrometry (MS) analyses to be present on EL4 cells but not on B6 thymocytes: VAAANREVL (*Xlr3*), SMYVPGKL (*Pfnd5*), STLTYSRM (*Sgk*) and NSMVLFDHV (*Top2a*) (Table 1) [32]. Genes coding for these LAAs were shown to be involved in several types of cancer (Supplemental Table S1). We experimentally validated that (1) each of our Ags was presented by either $H2D^b$ or $H2K^b$ (Figure 1A); and (2) in each case, mice primed with Ag-pulsed DCs generated cytotoxic T cells that killed EL4 cells in vitro (Figure 1B). Thus, our 8 Ags were immunogenic and were presented at the surface of EL4 cells by a single MHC class I allotype.

Protective Antileukemic Responses Can be Generated by Some miHAs but None of the LAAs

First, we wished to evaluate whether immunization against individual Ags could protect mice against EL4 leukemia. Mice were primed twice (day -14 and -7) with DCs pulsed with the miHA or LAA of interest. On day 0, mice were injected with 5×10^5 EL4 cells, and were, thereafter, monitored daily. Mice that were paralyzed, moribund, or presented tumors with a diameter greater than 1 cm were euthanized. B10-congeneic mice were primed against miHAs and B6 mice were primed against LAAs. We previously reported that disparity at the H9 locus between B10 and B6 mice had no effect on their respective response to EL4 cell injection [40,41]. Control mice were immunized with unpulsed syngeneic DCs.

Immunization against the $H4^a$ miHA and the 4 LAAs had no biologically significant effect on mice survival: all mice had to be sacrificed by day 29. For $H4^a$ and 3 LAAs, median survival was similar to that of control animals immunized with unpulsed DCs; for the SMYVPGKL LAA, immunization barely increased survival by 1.5 day (Figure 2). In contrast, priming against 3 other miHAs increased the mean survival to 29 days for $H13^a$ and to more than 100 days for $H3^a$ or $H7^a$. The protective value of anti-$H7^a$ responses was particularly impressive, as no death occurred before day 26 in unprimed $B10.H7^b$ mice and 60% remained leukemia-free at day 100 (Figure 2). To further hierarchize our Ags, we injected 5×10^4 EL4 cells (10-fold less than in the previous experiment) into mice immunized against the 6 Ags that did not generate complete protection against 5×10^5 EL4 cells. Immunization against the 4 individual LAAs and $H4^a$ had no or only marginal effect on mice survival (Supplemental Figure S1). By contrast, 40% of mice immunized against $H13^a$ remained leukemia-free on day 100 (Supplemental Figure S1). These data reveal the following hierarchy in the potency of antileukemic responses elicited by our 8 Ags: $H7^a > H3^a > H13^a >$ the 4 LAAs and $H4^a$. Accordingly, protective antileukemic responses were induced by 3 out of 4 miHAs but none of the LAAs.

Frequency of miHA- and LAA-specific CD8 T Cells in Immunized Mice

Next, we assessed T cell expansion after Ag priming using 2 methods: tetramer staining and IFN-γ ELISpot. These analyses were performed on FACS-sorted CD8 T cells from naïve and immunized mice. Mice immunized against $H7^a$, $H3^a$ and $H13^a$ showed conspicuous accumulation of tetramer-positive CD8 T cells (Figure 3A,B). For $H4^a$ and 3 LAAs, no tetramer$^+$ cells were detected, while in the case of VAAANREVL, a few tetramer$^+$ cells were observed.

In IFN-γ ELISpot assays, the mean frequency of SFCs per 10^6 CD8 T cells was 16,380 for $H7^a$, 12,440 for $H3^a$ and 4,827 for $H13^a$ (Figure 3C,D). For $H4^a$ and the 4 LAAs, the frequency of SFCs was less than 1,000 per 10^6 CD8 T cells. Thus, the Ag hierarchy in ELISpot assays was consistent with the hierarchy observed using tetramer staining (Figure 4A). Furthermore, the frequency of Ag-specific T cells detected with tetramer staining and IFN-γ ELISpot showed a strong correlation with mice survival after injection of EL4 cells (Figure 4B,C). The salient finding is, therefore, that the amplitude of T cell expansion correlates with the strength of antileukemic responses. Of note, for the 3 most immunogenic Ags ($H7^a$, $H3^a$, and $H13^a$), the number of cells labeled by tetramers (11,337 to 65,295 per 10^6 CD8 T cells) was about 3-fold greater than the number of IFN-γ producing cells (4827 to 16,380 per 10^6 CD8 T cells). In contrast, with the other Ags, the frequency of SFCs was similar (VAAANREVL) or greater ($H4^a$ and 3 LAAs) than the frequency tetramer$^+$ cells (Figures 3, 4). Tetramer staining can detect T cells with medium- to high-affinity TCRs. CD8 T cells with low-affinity TCRs are not stained by pMHC tetramers but can be detected with functional assays such as the IFN-γ ELISpot [42-44]. Our data, therefore, suggest that TCRs recognizing $H7^a$, $H3^a$, and $H13^a$ had higher affinity for pMHC than TCRs recognizing other Ags.

Antileukemic Activity Correlates with T Cell Functional Avidity

Having identified 3 immunodominant Ags that were able to induce protective antileukemic responses, we sought to determine the mechanism responsible for their dominance. As pointed out by Bihl et al., the term *immunodominance* is as widely used as it is loosely defined [45]. This is largely because the immunodominance hierarchy may vary as a function of the

Table 1
Key Features of miHA and LAAs

Antigen Type	Peptide Sequence	Peptide Source Gene	MHC I Allele	Predicted Binding Score (Nm)*	Reference
miHAs	**A**SP**C**NSTVL ($H3^a$) **T**SP**R**NSTVL ($H3^b$)	*Zfp106*	$H2D^b$	5.53	[34]
	SG**T**VYIHL ($H4^a$) SG**I**VYIHL ($H4^b$)	*Emp3*	$H2K^b$	60.06	[35]
	KAPDNR**E**TL ($H7^a$) KAPDNR**D**TL ($H7^b$)	*Stt3b*	$H2D^b$	37.51	[36,37]
	SSV**V**GVWYL ($H13^a$) SSV**I**GVWYL ($H13^b$)	*H13*	$H2D^b$	73.76	[38,39]
LAAs	NSMVLFDHV	*Top2a*	$H2D^b$	466.68	[32]
	VAAANREVL	*Xlr3a*	$H2D^b$	16.48	[32]
	SMYVPGKL	*Pfdn5*	$H2K^b$	146.63	[32]
	STLTYSRM	*Sgk1*	$H2K^b$	12.44	[32]

miHA indicates minor histocompatibility antigens; LAAs, leukemia-associated antigens.
* Predicted MHC binding score was determined using NetMHCCons.

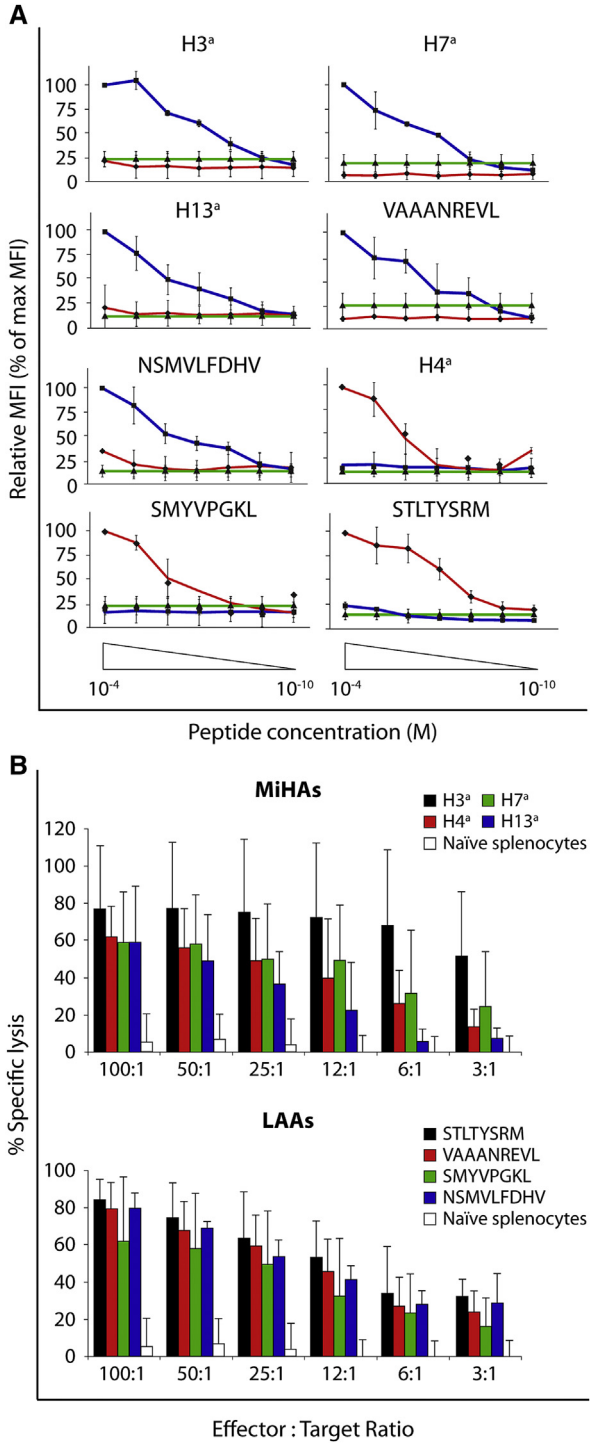

Figure 1. LAAs and miHAs are immunogenic and bind to a single MHC class I allotype. (A) Binding of LAAs and miHAs to $H2D^b$ and $H2K^b$. RMA-S cells were pulsed with graded concentrations of the relevant peptide and stained with Ab against $H2D^b$ (blue) or $H2K^b$ (red). As a negative control (green), unpulsed RMA-S cells were stained with Ab recognizing the relevant H2 allotype ($H2D^b$ or $H2K^b$). The relative binding (y axis) was calculated by normalizing the MFI obtained with each peptide concentration (x axis) to the intensity obtained at a peptide concentration of 10^{-4} M. (B) Cytotoxic T lymphocytes primed against individual miHAs and LAAs kill EL4 cells in vitro. Mice were immunized twice (day -14 and -7) with peptide-pulsed DCs. We used B6 mice for LAAs and B10-congeneic mice expressing the miHA *b* allele for the miHAs. On day 0, splenocytes from naïve and from immunized mice were depleted of NK cells and restimulated in vitro with peptide (2 μM) for 5 days. The resulting effector cells were incubated at different effector: target ratios with CFSE-stained EL4 target cells (x axis). All data are representative of 3 independent replicates.

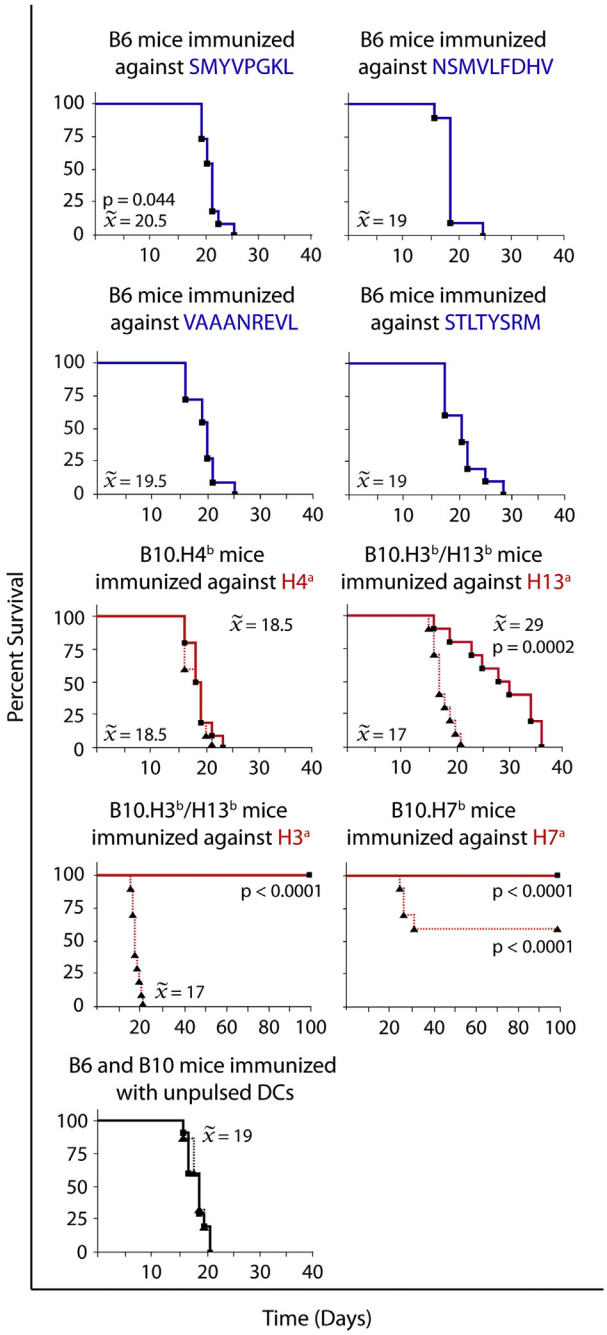

Figure 2. Mice immunized against miHAs are more resistant to EL4 cells than mice immunized against LAAs. B6 (solid blue line) or B10-congeneic (solid red line) mice were immunized with peptide-pulsed DCs on day -14 and -7, and received 5×10^5 EL4 cells i.v. on day 0. In control groups, EL4 cells were injected into B6 (solid black line), B10 (black dotted line) and B10-congeneic (red dotted line) mice immunized with unpulsed DCs. $\tilde{x}$ represents the median survival time. The log-rank test was used to compare the survival of various groups to that of B6 or B10 mice immunized with unpulsed DCs. Ten to 15 mice per group.

criteria used to build the hierarchy [46]. Here, we established our Ag hierarchy as a function of their ability to generate protective antileukemic responses (Figure 1, Supplemental Figure S1): $H7^a > H3^a > H13^a >$ the 4 LAAs and $H4^a$. This hierarchy was congruent with the number of Ag-specific T cells found after immunization (Figure 3). We then analyzed the factors associated with immunodominance in various

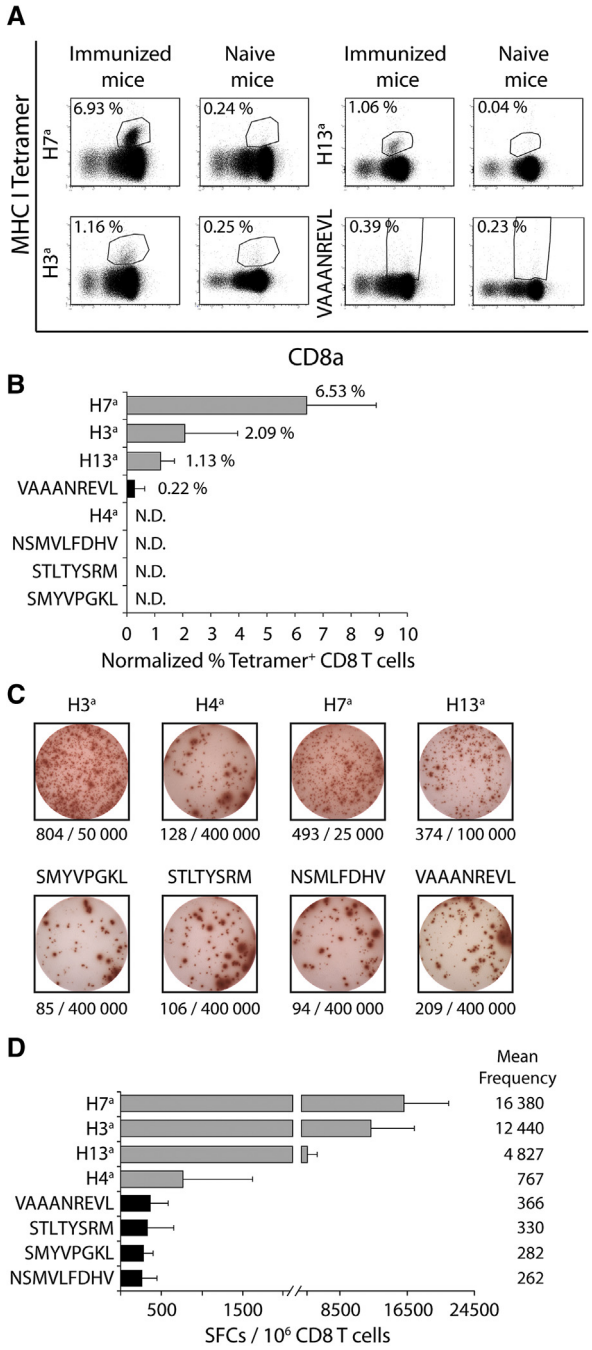

Figure 3. Frequency of Ag-specific CD8 T cells in primed mice. B6 or B10-congeneic mice were immunized twice with peptide-pulsed DCs (day -14 and -7). On day 0, splenocytes were harvested from the spleen of 3 naïve and 3 immunized mice (B6 mice for LAAs and B10-congeneic mice expressing the *b* allele for the miHAs). Splenocytes were stained with anti-CD8a Ab and sorted by fluorescence-activated cell sorting. (A and B) Sorted CD8 T cells were stained with MHC class I tetramers. (A) One representative experiment. (B) Frequency of tetramer$^+$ elements among CD8 T cells. Specific tetramer staining was obtained by subtracting the unspecific staining observed in naïve unprimed mice. N.D. indicates not detected. Data represent the mean percentage of tetramer$^+$ cells. Four to 5 independent experiments per Ag. The frequencies of tetramer$^+$ T cells was significantly higher for H7^a, H3^a, and H13^a than for other Ags ($P < .05$; *t*-test). (C and D) Sorted CD8 T cells were plated on a MultiScreen PVDF plate and incubated for 48 hours in the presence of irradiated peptide-pulsed splenocytes. SFCs were counted using an ImmunoSpot analyzer. (C) One representative experiment. The number of spot forming cells and the number of plated CD8 T cells are indicated below each well. (D) The frequency of SFCs in primed mice was calculated by subtracting the number of SFCs in naïve mice. Data are expressed as the mean frequency of SFCs per 10^6 CD8 T cells plated (3 independent experiments).

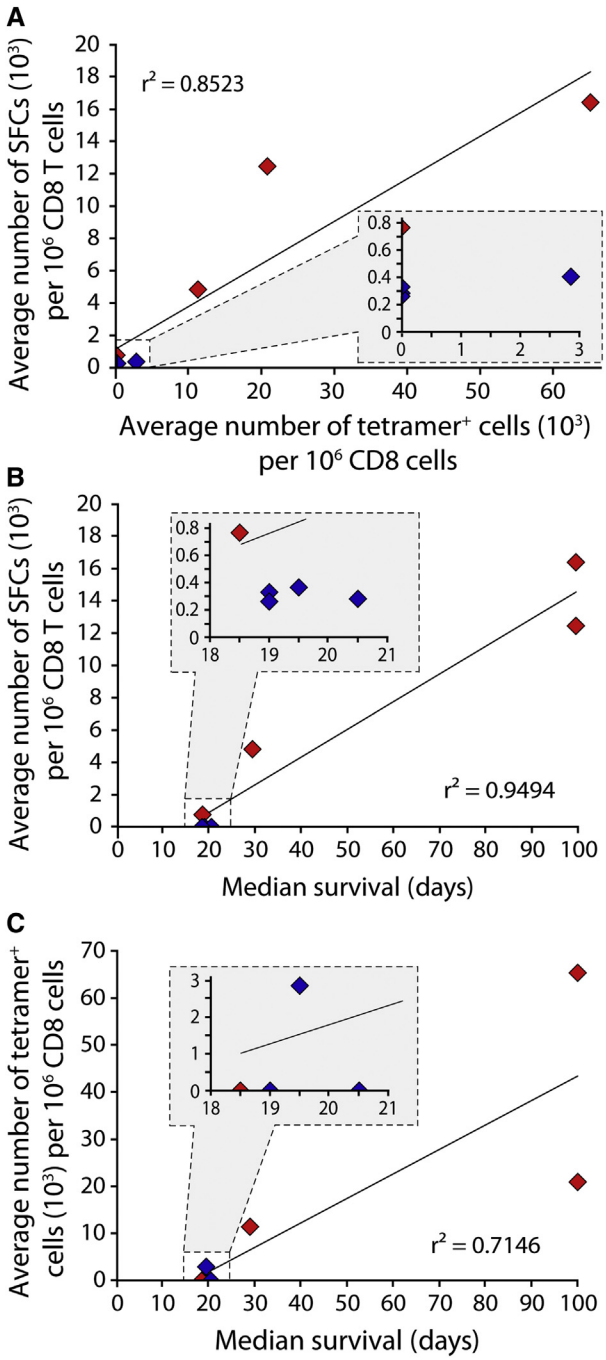

Figure 4. The frequency of Ag-specific CD8 T cells in immunized mice correlates with survival. (A) Correlation between the frequencies of SFCs (IFN-γ ELISpot) and of tetramer$^+$ T cells. Correlation between median survival and (B) the frequencies of SFCs (IFN-γ ELISpot) and of (C) tetramer$^+$ T cells. Fitness of curves was determined by the coefficient of determination (r^2). miHAs are represented in red, LAAs in blue. Grey inserts show zoomed in depiction of low values.

experimental models, including properties of the Ag (density on target cells, MHC binding affinity, and stability of pMHC complexes) and of cognate T cells (frequency and functional avidity) [31,47-59].

Epitope Density on EL4 Cells

MHC I-associated peptides were eluted from the cell surface of EL4 cells, spiked with ^{13}C-labeled synthetic

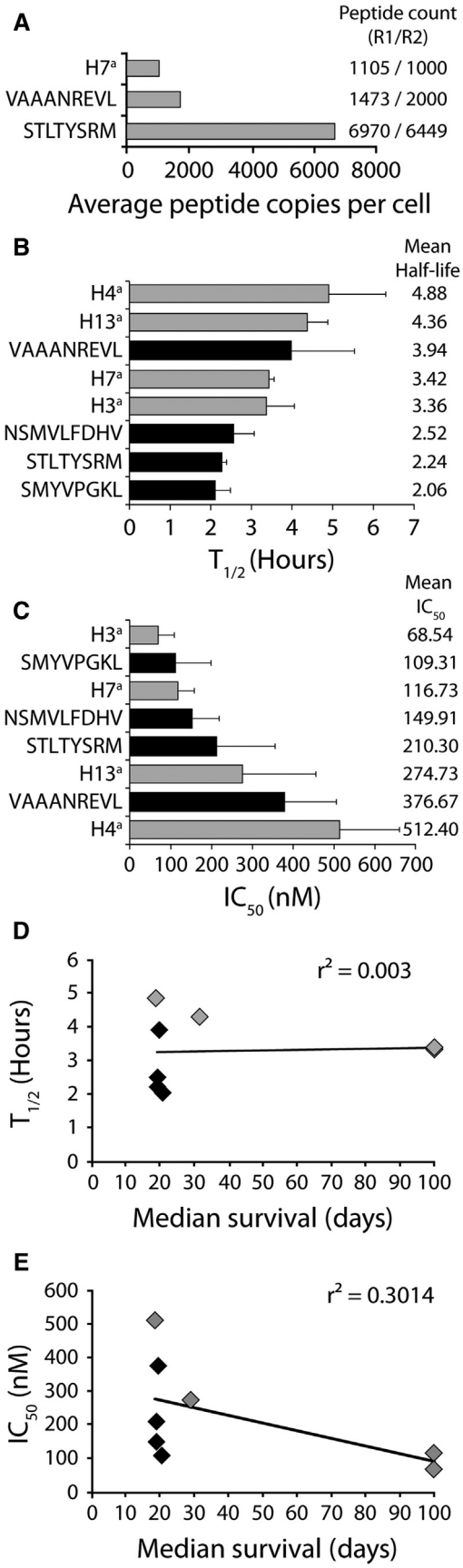

Figure 5. Epitope stability and abundance on EL4 cells do not correlate with Ag potency. (A) Peptide abundance at the surface of EL4 cells. The abundance of H7[a], VAAANREVL, and STLTYSRM was measured by MS. Two biological replicates (R1 and R2) per peptide. (B) Half-life of pMHC complexes. RMA-S cells were incubated overnight with 50 μM of the selected peptide. Cells were then washed, incubated at 37°C and chased every hour for 12 hours by staining for either $H2D^b$ or $H2K^b$. The half-life of the top 5 Ags was longer than that of STLTYSRM and SMYVPGKL ($P < .05$; *t*-test). (C) Peptide binding affinity was determined by a competition-based peptide-binding assay. RMA-S cells were pulsed with peptide concentrations ranging from 10^{-10} to 10^{-4} M and with 10^{-7} M of (ASP[Lys-FITC]NSTVL) ($H3^a$) for $H2D^b$ binding peptides or (SII [Lys-FITC]FEKL) for $H2K^b$ binding peptides. Data were normalized to maximum intensity values. The top 4 Ags showed a greater MHC binding affinity than VAAANREVL and $H4^a$ ($P < .05$; *t*-test). However, statistical analysis showed no significant differences between miHAs (grey) and LAAs (black). Half-life of pMHC complexes (D) and peptide binding affinity (E) were plotted against the median survival of EL4 bearing mice. Fitness of the curves was determined by the coefficient of determination (r^2).

peptides, fractionated by liquid chromatography and analyzed by MS for detection of isotopomers. Isotopomers (peptides that have the same sequence but differ by the presence of 1 isotopically labelled atom), appear as coeluting pairs with a defined mass difference [28,60]. Absolute quantification of peptide abundance was achieved by comparing the abundance of native peptides to their corresponding ^{13}C-synthetic analogs. Three peptides were selected for analysis: $H7^a$ which stands at the top of the hierarchy, and 2 LAAs, which are at the bottom of the hierarchy (VAAANREVL and STLTYSRM). Of note, based on the NetMHCCons algorithm [61], these 3 peptides were predicted to have high MHC binding scores (Table 1). The mean number of peptide copies per EL4 cell was estimated to be 1053 for $H7^a$, 1737 for VAAANREVL and 6710 for STLTYSRM (Figure 5A). Thus, the abundance of $H7^a$ was in no way remarkable, being lower than that of the 2 LAAs. Hence, epitope abundance on target EL4 cells did not correlate with immunodominance.

MHC Binding Affinity and Stability of pMHC Complexes

For the assessment of the half-life of pMHC complexes, RMA-S cells were incubated at 26°C overnight with the selected peptide. Cells were then washed, incubated at 37°C, and analyzed by flow cytometry every hour for 12 hours for expression of $H2D^b$ or $H2K^b$. The half-life of pMHC complexes, determined by using a 1-phase exponential decay equation, ranged from 2.06 hours to 4.88 hours (Figure 5B). To evaluate the MHC binding affinity of our 8 peptides, we performed a competition-based assay using FITC-labeled synthetic peptides [30]. We compared the ability of $H2D^b$ and $H2K^b$ binding peptides to displace either (ASP[Lys-FITC] NSTVL) ($H3^a$) or (SII[Lys-FITC]FEKL), respectively. We validated that FITC-conjugation of the reference peptides did not prevent binding to their respective MHC allotype (data not shown). The peptide concentration required for half-maximal displacement of the FITC-conjugated peptide was determined using a dose-response curve and ranged from 68.54 to 512.40 nM for (Figure 5C). The MHC binding affinity and stability of pMHC complexes did not correlate with the strength of antileukemic responses (Figure 5D,E). For both parameters we observed a major overlap between immunodominant and immunorecessive epitopes (Figure 5B,C).

T Cell Functional Avidity

If immunodominance in our model is not dictated by properties of the Ags per se, it must be dictated by properties of their cognate T cells: T cell frequency in the preimmune repertoire or T cell functional avidity [57,58,62]. Frequencies

of Ag-specific T cells in the preimmune repertoire range from 1 to 89 cells/million naïve CD8 T cells [57]. That the frequency of H7^a-specific T cells lies at the lower end of this range (at 2 cells/million) [31] argues against the possibility that our immunodominant Ags are recognized by high-frequency CD8 T cells. We, therefore, investigated the role of functional avidity of Ag-specific T cells using serial peptide concentrations and defining EC_{50} as the exogenous peptide concentration yielding half-maximal counts in IFN-γ ELISpot assays. In these assays, functional avidity (or antigen sensitivity) of CD8 T cells refers to their activation threshold in response to defined concentrations of exogenous peptide [54,63]. We were unable to assess the frequency of T cells specific for H4^a and the 4 LAAs because their frequency was too low (Figure 3D). Nonetheless, we found that the EC_{50} for H7^a, H3^a, and H13^a (the 3 top Ags) were .28 nM, 11.35 nM and 32.02 nM, respectively (Figure 6A). Functional avidity showed a strong correlation with antileukemic activity (Figure 6B).

DISCUSSION

Our work provides a direct comparison of antileukemic responses elicited by individual miHAs and LAAs. We wish to reiterate that the 8 Ags studied herein were shown to be present on EL4 cells [32,34-39] and each of them elicited CD8 T cells responses detectable by ELISpot and cytotoxicity assays. Furthermore, for priming mice against specific Ags before challenge with EL4 cells, we used DCs pulsed with the same peptide concentration (2 μM) in each case. Thus, we strived to minimize any potential bias toward miHAs or LAAs and, a priori, our 8 Ags might have been considered potential targets for leukemia immunotherapy. This was definitely not the case, and we posit that several points can be made from our study.

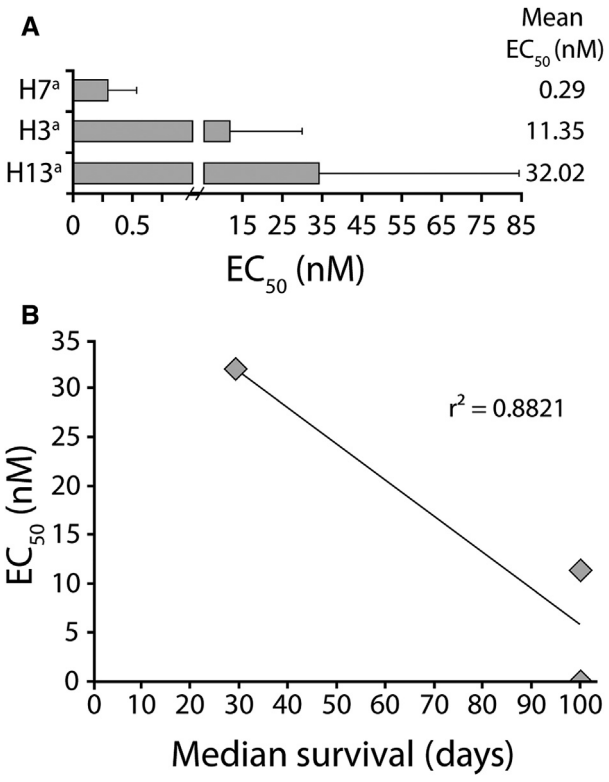

Figure 6. T cell functional avidity correlates with Ag potency. Sorted CD8 T cells were plated on a MultiScreen PVDF plate and incubated for 48 hours in the presence of peptide-pulsed (10^{-4} to 10^{-14} M) irradiated splenocytes. SFCs were counted using an ImmunoSpot analyzer. (A) Data were normalized to maximum intensity value and plotted using dose-response curves to determine the EC_{50} of each peptide (3 independent experiments). The functional avidity of H7^a-specific T cells was superior to that of H3^a and H13^a-specific T cells ($P < .05$) (B) Average avidity was plotted against the median survival following injection of EL4 cells. Fitness of curves was determined by the coefficient of determination (r^2).

One clear conclusion is that the mere expression of a given Ag on the surface of leukemic cell and its ability to elicit IFN-γ secretion and cytotoxic responses (in vitro) are insufficient to predict that the Ag will elicit expansion of tetramer$^+$ T cells and biologically relevant T cell responses in vivo. That was the case for our 4 LAAs and 1 miHA (H4^a). In vitro ELISpot and cytotoxicity assays are very sensitive and may pick up biologically irrelevant responses from tetramer-negative T cells [59,64]. Indeed, CD8 T cells that respond specifically to pMHC on target cells (in vitro), yet are not stained by the same pMHC as tetramers, have been reported in several studies [42,65-67]. These in vitro responsive but tetramer-negative CD8 T cells were shown to display low TCR-pMHC affinity and, therefore, to be functionally inferior to tetramer$^+$ T cells in vivo [43,59]. Other negative findings relate to pMHC interactions: miHAs and LAAs had overlapping affinities for their cognate MHC molecule, and neither peptide affinity nor the stability of pMHC complexes correlated with the strength of T cell responses. Because absolute peptide quantification by MS is not widely available, very little is known on the expression of miHAs and LAAs at the peptide level (as opposed to the transcript or protein level) [68].

Somewhat unexpectedly, we found that peptide density on leukemic cells did not correlate with the ability of primed T cells to eliminate leukemic cells. The abundance of H7^a (the best Ag) was inferior to that of the 2 LAAs, which elicited no antileukemic response (Figure 5A). Thus, at the effector stage, epitope density on target cells was not a critical parameter. This is consistent with the fact that killing of target cells by effector CD8 T cells only requires 3 pMHC complexes/target cell, and that the delivery of lytic granules to target cells is rapid and insensitive to Ag density [59,69,70].

In our model, LAAs were clearly inferior to miHAs as targets for immunotherapy. The most parsimonious explanation is that high avidity T cells are deleted from the T cell repertoire specific for self Ags (LAAs) but not for allo-Ags (miHAs). However, it would be premature to dismiss all LAAs from future studies. There are 3 main classes of LAAs: those that are overexpressed on leukemic relative to normal cells, cancer-testis Ags, and leukemia-specific Ags derived from cancer-specific somatic mutations. Our conclusions strictly concern LAAs that are overexpressed on leukemic cells relative to normal cells. Overexpressed Ags nonetheless represent the largest class of LAAs (eg, WT1, PR1, hTERT) and the class that has received most attention because these Ags are present on leukemic cells in most patients [1]. Cancer-testis Ags are attractive because they are shared by many tumors and were thought to be expressed only in tissues that do not express MHC molecules and cannot, therefore, induce central tolerance. However, more refined studies have revealed expression of cancer-testis Ags in several cell subsets, including medullary thymic epithelial cells [71,72]. Furthermore, with 1 exception (cyclin-A1), cancer-testis Ags are poorly expressed by leukemic cells [73]. From an immunologic perspective, Ags derived from cancer mutations are extremely attractive because they are truly cancer specific and cannot induce canonical central tolerance.

However, 2 recent reports suggest that discovery of immunogenic leukemia-specific Ags will be extremely challenging and might be impossible for a large proportion of patients. Indeed, hematologic cancers have fewer mutations than other cancers (eg, an average of 13 mutations per acute myelogenous leukemia genome) [24], and only about 5% of cancer mutations yield immunogenic HLA class I-associated epitopes [74].

The number of potential antigenic targets (miHAs and LAAs) for T cell based leukemia immunotherapy is considerable. It would be impossible to evaluate in vivo the antileukemic potency of T cells targeted to all potential Ags. It is therefore imperative to establish reliable criteria for in vitro prediction of antileukemic activity. Of practical importance, we found that the best predictor of antileukemic efficacy measurable directly in vitro was T cell functional avidity. Functional avidity is determined mainly by TCR affinity for its cognate epitope: in some models the k_{on} of TCR-pMHC association is the key element, in others the k_{off} is more important [31,58,75]. Other factors may impinge on functional avidity including the expression level of TCRs, adhesion molecules or coreceptors, and changes in components of the signaling cascade. When dealing with polyclonal T cell populations (as opposed to single TCRs), it is difficult to decipher the underpinnings of differential functional avidity. Nonetheless, from a practical standpoint, our work suggests that in vitro evaluation of functional avidity represents the best criterion for selection of Ags, which should be prioritized in clinical trials of leukemia immunotherapy.

ACKNOWLEDGMENTS

We are grateful to the staff of the animal care, flow cytometry and proteomics IRIC core facilities for their assistance. The authors also thank the NIH tetramer core facility for providing reagents as well as Danielle de Verteuil, Moutih Rafei and Sébastien Lemieux for thoughtful comments.

Financial disclosure: The Institute for Research in Immunology and Cancer (IRIC) is supported in part by the Canada Foundation for Innovation and the Fonds de Recherche Santé Québec. K.V. holds a PhD studentship from the Canadian Institutes of Health Research, I.S.F. is a recipient of a PhD scholarship from le Fonds de la Recherche du Québec-Santé, and C.M.L. was supported by a studentship from the Défi Persévérance-Famille Gosselin Fund. C.P. and P.T. hold Canada Research Chairs in Immunobiology, and Proteomics and Bioanalytical Spectrometry, respectively. H.S. is supported by the Leukemia and Lymphoma Society of Canada and by La Fondation Centre de Cancérologie Charles-Bruneau. C.P.'s lab is supported in part by the Katelyn Bedard Bone Marrow Association. This study was funded by the Leukemia & Lymphoma Society of Canada.

Conflict of interest statement: There are no conflicts of interest to report.

SUPPLEMENTARY DATA

Supplementary data related to this article can be found at http://dx.doi.org/10.1016/j.bbmt.2013.10.020.

REFERENCES

1. Bleakley M, Riddell SR. Molecules and mechanisms of the graft-versus-leukaemia effect. *Nat Rev Cancer*. 2004;4:371-380.
2. Vincent K, Roy DC, Perreault C. Next-generation leukemia immunotherapy. *Blood*. 2011;118:2951-2959.
3. Jenq RR, van den Brink MR. Allogeneic haematopoietic stem cell transplantation: individualized stem cell and immune therapy of cancer. *Nat Rev Cancer*. 2010;10:213-221.
4. Hsieh MH, Patterson AE, Korngold R. T-cell subsets mediate graft-versus-myeloid leukemia responses via different cytotoxic mechanisms. *Biol Blood Marrow Transplant*. 2000;6:231-240.
5. Hsieh MH, Korngold R. Differential use of FasL- and perforin-mediated cytolytic mechanisms by T-cell subsets involved in graft-versus-myeloid leukemia responses. *Blood*. 2000;96:1047-1055.
6. Reddy P, Maeda Y, Liu C, et al. A crucial role for antigen-presenting cells and alloantigen expression in graft-versus-leukemia responses. *Nat Med*. 2005;11:1244-1249.
7. Schmaltz C, Alpdogan O, Kappel BJ, et al. T cells require TRAIL for optimal graft-versus-tumor activity. *Nat Med*. 2002;8:1433-1437.
8. Matte-Martone C, Liu J, Jain D, et al. $CD8^+$ but not $CD4^+$ T cells require cognate interactions with target tissues to mediate GVHD across only minor H antigens whereas both $CD4^+$ and $CD8^+$ T cells require direct leukemic contact to mediate GVL. *Blood*. 2008;111:3884-3892.
9. Spierings E, Drabbels J, Hendriks M, et al. A uniform genomic minor histocompatibility antigen typing methodology and database designed to facilitate clinical applications. *PLoS ONE*. 2006;1:e42.
10. Roopenian D, Choi EY, Brown A. The immunogenomics of minor histocompatibility antigens. *Immunol Rev*. 2002;190:86-94.
11. Spierings E, Hendriks M, Absi L, et al. Phenotype frequencies of autosomal minor histocompatibility antigens display significant differences among populations. *PLoS Genet*. 2007;3:e103.
12. Warren EH, Zhang XC, Li S, et al. Effect of MHC and non-MHC donor/recipient genetic disparity on the outcome of allogeneic HCT. *Blood*. 2012;120:2796-2806.
13. Pion S, Fontaine P, Baron C, et al. Immunodominant minor histocompatibility antigens expressed by mouse leukemic cells can serve as effective targets for T cell immunotherapy. *J Clin Invest*. 1995;95:1561-1568.
14. Hobo W, Broen K, van der Velden WJ, et al. Association of disparities in known minor histocompatibility antigens with relapse-free survival and graft-versus-host-disease after allogeneic stem cell transplantation. *Biol Blood Marrow Transplant*. 2013;19:274-282.
15. Broen K, Greupink-Draaisma A, Fredrix H, et al. Induction of multiple myeloma-reactive T cells during post-transplantation immunotherapy with donor lymphocytes and recipient DCs. *Bone Marrow Transplant*. 2012;47:1229-1234.
16. Hambach L, Goulmy E. Immunotherapy of cancer through targeting of minor histocompatibility antigens. *Curr Opin Immunol*. 2005;17:202-210.
17. Spierings E, Kim YH, Hendriks M, et al. Multicenter analyses demonstrate significant clinical effects of minor histocompatibility antigens on GvHD and GvL after HLA-matched related and unrelated hematopoietic stem cell transplantation. *Biol Blood Marrow Transplant*. 2013;19:1244-1253.
18. Hambach L, Nijmeijer BA, Aghai Z, et al. Human cytotoxic T lymphocytes specific for a single minor histocompatibility antigen HA-1 are effective against human lymphoblastic leukaemia in NOD/scid mice. *Leukemia*. 2006;20:371-374.
19. Hambach L, Vermeij M, Buser A, Aghai Z, van der Kwast T, Goulmy E. Targeting a single mismatched minor histocompatibility antigen with tumor-restricted expression eradicates human solid tumors. *Blood*. 2008;112:1844-1852.
20. Molldrem JJ, Lee PP, Wang C, et al. Evidence that specific T lymphocytes may participate in the elimination of chronic myelogenous leukemia. *Nat Med*. 2000;6:1018-1023.
21. Rezvani K, Yong AS, Savani BN, et al. Graft-versus-leukemia effects associated with detectable Wilms tumor-1 specific T lymphocytes after allogeneic stem-cell transplantation for acute lymphoblastic leukemia. *Blood*. 2007;110:1924-1932.
22. Lindahl KF. Minor histocompatibility antigens. *Trends Genet*. 1991;7:219-224.
23. Dupage M, Mazumdar C, Schmidt LM, et al. Expression of tumour-specific antigens underlies cancer immunoediting. *Nature*. 2012;482:405-409.
24. The Cancer Genome Atlas Research Network. Genomic and epigenomic landscapes of adult de novo acute myeloid leukemia. *N Engl J Med*. 2013;368:2059-2074.
25. van den Brink MR, Porter DL, Giralt S, et al. Relapse after allogeneic hematopoietic cell therapy. *Biol Blood Marrow Transplant*. 2010;16:S138-S145.
26. Miller JS, Warren EH, van den Brink MR, et al. NCI First International Workshop on The Biology, Prevention, and Treatment of Relapse After Allogeneic Hematopoietic Stem Cell Transplantation: Report from the Committee on the Biology Underlying Recurrence of Malignant Disease following Allogeneic HSCT: graft-versus-tumor/leukemia reaction. *Biol Blood Marrow Transplant*. 2010;16:565-586.
27. de Verteuil D, Muratore-Schroeder TL, Granados DP, et al. Deletion of immunoproteasome subunits imprints on the transcriptome and has a broad impact on peptides presented by major histocompatibility complex I molecules. *Mol Cell Proteomics*. 2010;9:2034-2047.
28. Caron E, Vincent K, Fortier MH, et al. The MHC I immunopeptidome conveys to the cell surface an integrative view of cellular regulation. *Mol Syst Biol*. 2011;7:533.

29. Rock KL, Gramm C, Benacerraf B. Low temperature and peptides favor the formation of class I heterodimers on RMA-S cells at the cell surface. *Proc Natl Acad Sci U S A*. 1991;88:4200-4204.
30. Kessler JH, Mommaas B, Mutis T, et al. Competition-based cellular peptide binding assays for 13 prevalent HLA class I alleles using fluorescein-labeled synthetic peptides. *Hum Immunol*. 2003;64: 245-255.
31. Roy-Proulx G, Baron C, Perreault C. CD8 T-cell ability to exert immunodomination correlates with T-cell receptor:epitope association rate. *Biol Blood Marrow Transplant*. 2005;11:260-271.
32. Fortier MH, Caron E, Hardy MP, et al. The MHC class I peptide repertoire is molded by the transcriptome. *J Exp Med*. 2008;205:595-610.
33. Tan CT, Croft NP, Dudek NL, et al. Direct quantitation of MHC-bound peptide epitopes by selected reaction monitoring. *Proteomics*. 2011; 11:2336-2340.
34. Zuberi AR, Christianson GJ, Mendoza LM, et al. Positional cloning and molecular characterization of an immunodominant cytotoxic determinant of the mouse H3 minor histocompatibility complex. *Immunity*. 1998;9:687-698.
35. Yadav R, Yoshimura Y, Boesteanu A, et al. The $H4^{b}$ minor histocompatibility antigen is caused by a combination of genetically determined and posttranslational modifications. *J Immunol*. 2003;170:5133-5142.
36. Eden PA, Christianson GJ, Fontaine P, et al. Biochemical and immunogenetic analysis of an immunodominant peptide ($B6^{dom1}$) encoded by the classical H7 minor histocompatibility locus. *J Immunol*. 1999;162: 4502-4510.
37. McBride K, Baron C, Picard S, et al. The model $B6^{dom1}$ minor histocompatibility antigen is encoded by a mouse homolog of the yeast STT3 gene. *Immunogenetics*. 2002;54:562-569.
38. Mendoza LM, Paz P, Zuberi A, et al. Minors held by majors: the H13 minor histocompatibility locus defined as a peptide-MHC class I complex. *Immunity*. 1997;7:461-472.
39. Ostrov DA, Roden MM, Shi W, et al. How H13 histocompatibility peptides differing by a single methyl group and lacking conventional MHC binding anchor motifs determine self-nonself discrimination. *J Immunol*. 2002;168:283-289.
40. Roderick TH, Guidi JN. Strain distribution of polymorphic variants. In: Lyon MF, Searle AG, editors. *Genetic variants and strains of the laboratory mouse*. Oxford: Oxford University Press; 1989. p. 663-772.
41. Fontaine P, Roy-Proulx G, Knafo L, et al. Adoptive transfer of T lymphocytes targeted to a single immunodominant minor histocompatibility antigen eradicates leukemia cells without causing graft-versus-host disease. *Nat Med*. 2001;7:789-794.
42. Laugel B, van den Berg HA, Gostick E, et al. Different T cell receptor affinity thresholds and CD8 coreceptor dependence govern cytotoxic T lymphocyte activation and tetramer binding properties. *J Biol Chem*. 2007;282:23799-23810.
43. Stone JD, Artyomov MN, Chervin AS, et al. Interaction of streptavidin-based peptide-MHC oligomers (tetramers) with cell-surface TCRs. *J Immunol*. 2011;187:6281-6290.
44. Davis MM, Altman JD, Newell EW. Interrogating the repertoire: broadening the scope of peptide-MHC multimer analysis. *Nat Rev Immunol*. 2011;11:551-558.
45. Bihl F, Frahm N, Di Giammarino L, et al. Impact of HLA-B alleles, epitope binding affinity, functional avidity, and viral coinfection on the immunodominance of virus-specific CTL responses. *J Immunol*. 2006; 176:4094-4101.
46. Gallimore A, Dumrese T, Hengartner H, et al. Protective immunity does not correlate with the hierarchy of virus- specific cytotoxic T cell responses to naturally processed peptides. *J Exp Med*. 1998;187: 1647-1657.
47. Busch DH, Pamer EG. MHC class I/peptide stability: implications for immunodominance, in vitro proliferation, and diversity of responding CTL. *J Immunol*. 1998;160:4441-4448.
48. Pion S, Christianson GJ, Fontaine P, et al. Shaping the repertoire of cytotoxic T-lymphocyte responses: explanation for the immunodominance effect whereby cytotoxic T lymphocytes specific for immunodominant antigens prevent recognition of nondominant antigens. *Blood*. 1999;93:952-962.
49. Wherry EJ, Puorro KA, Porgador A, Eisenlohr LC. The induction of virus-specific CTL as a function of increasing epitope expression: responses rise steadily until excessively high levels of epitope are attained. *J Immunol*. 1999;163:3735-3745.
50. Yewdell JW, Bennink JR. Immunodominance in major histocompatibility complex class I-restricted T lymphocyte responses. *Annu Rev Immunol*. 1999;17:51-88.
51. Bullock TN, Colella TA, Engelhard VH. The density of peptides displayed by dendritic cells affects immune responses to human tyrosinase and gp100 in HLA-A2 transgenic mice. *J Immunol*. 2000;164:2354-2361.
52. Derby MA, Alexander-Miller MA, Tse R, Berzofsky JA. High-avidity CTL exploit two complementary mechanisms to provide better protection against viral infection than low-avidity CTL. *J Immunol*. 2001;166: 1690-1697.
53. Roy-Proulx G, Meunier MC, Lanteigne AM, et al. Immunodomination results from functional differences between competing CTL. *Eur J Immunol*. 2001;31:2284-2292.
54. Almeida JR, Sauce D, Price DA, et al. Antigen sensitivity is a major determinant of $CD8^{+}$ T-cell polyfunctionality and HIV-suppressive activity. *Blood*. 2009;113:6351-6360.
55. Moutaftsi M, Salek-Ardakani S, Croft M, et al. Correlates of protection efficacy induced by vaccinia virus-specific $CD8^{+}$ T-cell epitopes in the murine intranasal challenge model. *Eur J Immunol*. 2009;39:717-722.
56. Berger CT, Frahm N, Price DA, et al. High-functional-avidity cytotoxic T lymphocyte responses to HLA-B-restricted Gag-derived epitopes associated with relative HIV control. *J Virol*. 2011;85:9334-9345.
57. Jenkins MK, Moon JJ. The role of naïve T cell precursor frequency and recruitment in dictating immune response magnitude. *J Immunol*. 2012;188:4135-4140.
58. Nauerth M, Weissbrich B, Knall R, et al. TCR-ligand k_{off} rate correlates with the protective capacity of antigen-specific CD8+ T cells for adoptive transfer. *Sci Transl Med*. 2013;5:192ra87.
59. Zhong S, Malecek K, Johnson LA, et al. T-cell receptor affinity and avidity defines antitumor response and autoimmunity in T-cell immunotherapy. *Proc Natl Acad Sci U S A*. 2013;110:6973-6978.
60. Granados DP, Yahyaoui W, Laumont CM, et al. MHC I-associated peptides preferentially derive from transcripts bearing miRNA recognition elements. *Blood*. 2012;119:e181-e191.
61. Karosiene E, Lundegaard C, Lund O, Nielsen M. NetMHCcons: a consensus method for the major histocompatibility complex class I predictions. *Immunogenetics*. 2012;64:177-186.
62. Kotturi MF, Scott I, Wolfe T, et al. Naive precursor frequencies and MHC binding rather than the degree of epitope diversity shape $CD8^{+}$ T cell immunodominance. *J Immunol*. 2008;181:2124-2133.
63. Almeida JR, Price DA, Papagno L, et al. Superior control of HIV-1 replication by $CD8^{+}$ T cells is reflected by their avidity, polyfunctionality, and clonal turnover. *J Exp Med*. 2007;204:2473-2485.
64. Perreault C, Roy DC, Fortin C. Immunodominant minor histocompatibility antigens: the major ones. *Immunol Today*. 1998;19:69-74.
65. Burrows SR, Kienzle N, Winterhalter A, Bharadwaj M, Altman JD, Brooks A. Peptide-MHC class I tetrameric complexes display exquisite ligand specificity. *J Immunol*. 2000;165:6229-6234.
66. Buslepp J, Zhao R, Donnini D, et al. T cell activity correlates with oligomeric peptide-major histocompatibility complex binding on T cell surface. *J Biol Chem*. 2001;276:47320-47328.
67. Hernandez J, Lee PP, Davis MM, Sherman LA. The use of HLA A2.1/p53 peptide tetramers to visualize the impact of self tolerance on the TCR repertoire. *J Immunol*. 2000;164:596-602.
68. de Verteuil D, Granados DP, Thibault P, Perreault C. Origin and plasticity of MHC I-associated self peptides. *Autoimmun Rev*. 2012;11: 627-635.
69. Purbhoo MA, Irvine DJ, Huppa JB, Davis MM. T cell killing does not require the formation of a stable mature immunological synapse. *Nat Immunol*. 2004;5:524-530.
70. Wiedemann A, Depoil D, Faroudi M, Valitutti S. Cytotoxic T lymphocytes kill multiple targets simultaneously via spatiotemporal uncoupling of lytic and stimulatory synapses. *Proc Natl Acad Sci U S A*. 2006; 103:10985-10990.
71. Morgan RA, Chinnasamy N, Abate-Daga D, et al. Cancer regression and neurological toxicity following anti-MAGE-A3 TCR gene therapy. *J Immunother*. 2013;36:133-151.
72. St-Pierre C, Brochu S, Vanegas JR, et al. Transcriptome sequencing of neonatal thymic epithelial cells. *Sci Rep*. 2013;3:1860.
73. Ochsenreither S, Majeti R, Schmitt T, et al. Cyclin-A1 represents a new immunogenic targetable antigen expressed in acute myeloid leukemia stem cells with characteristics of a cancer-testis antigen. *Blood*. 2012; 119:5492-5501.
74. Robbins PF, Lu YC, El-Gamil M, et al. Mining exomic sequencing data to identify mutated antigens recognized by adoptively transferred tumor-reactive T cells. *Nat Med*. 2013;19:747-752.
75. Aleksic M, Dushek O, Zhang H, et al. Dependence of T cell antigen recognition on T cell receptor-peptide MHC confinement time. *Immunity*. 2010;32:163-174.